



Published in final edited form as:

Cell Rep. 2023 March 28; 42(3): 112143. doi:10.1016/j.celrep.2023.112143.

## Notch-dependent binary fate choice regulates the Netrin pathway to control axon guidance of *Drosophila* visual projection neurons

Yu Zhang<sup>1</sup>, Scott Lowe<sup>1</sup>, Andrew Z. Ding<sup>1</sup>, Xin Li<sup>1,2,\*</sup>

<sup>1</sup>Department of Cell and Developmental Biology, University of Illinois Urbana-Champaign, Urbana, IL 61801, USA

<sup>2</sup>Lead contact

### SUMMARY

Notch-dependent binary fate choice between sister neurons is one of the mechanisms to generate neural diversity. How these upstream neural fate specification programs regulate downstream effector genes to control axon targeting and neuropil assembly remains less well understood. Here, we report that Notch-dependent binary fate choice in *Drosophila* medulla neurons is required to regulate the Netrin axon guidance pathway, which controls targeting of transmedullary (Tm) neurons to lobula. In medulla neurons of Notch-on hemilineage composed of mostly lobula-targeting neurons, Notch signaling is required to activate the expression of Netrin-B and repress the expression of its repulsive receptor Unc-5. Turning off Unc-5 is necessary for Tm neurons to target lobula. Furthermore, Netrin-B provided by Notch-on medulla neurons is required for correct targeting of Tm axons from later-generated medulla columns. Thus, the coordinate regulation of Netrin pathway components by Notch signaling ensures correct targeting of Tm axons and contributes to the neuropil assembly.

### In brief

Sister neurons adopt distinct fates because of different Notch signaling status. Zhang et al. find that in neurons of the *Drosophila* optic lobe, Notch signaling activates the expression of Netrin, an axon guidance cue, and represses the expression of Unc5, its repulsive receptor, to control axon guidance and neuropil assembly.

### Graphical Abstract

---

This is an open access article under the CC BY-NC-ND license (<http://creativecommons.org/licenses/by-nc-nd/4.0/>).

\*Correspondence: [lixin@illinois.edu](mailto:lixin@illinois.edu).

#### AUTHOR CONTRIBUTIONS

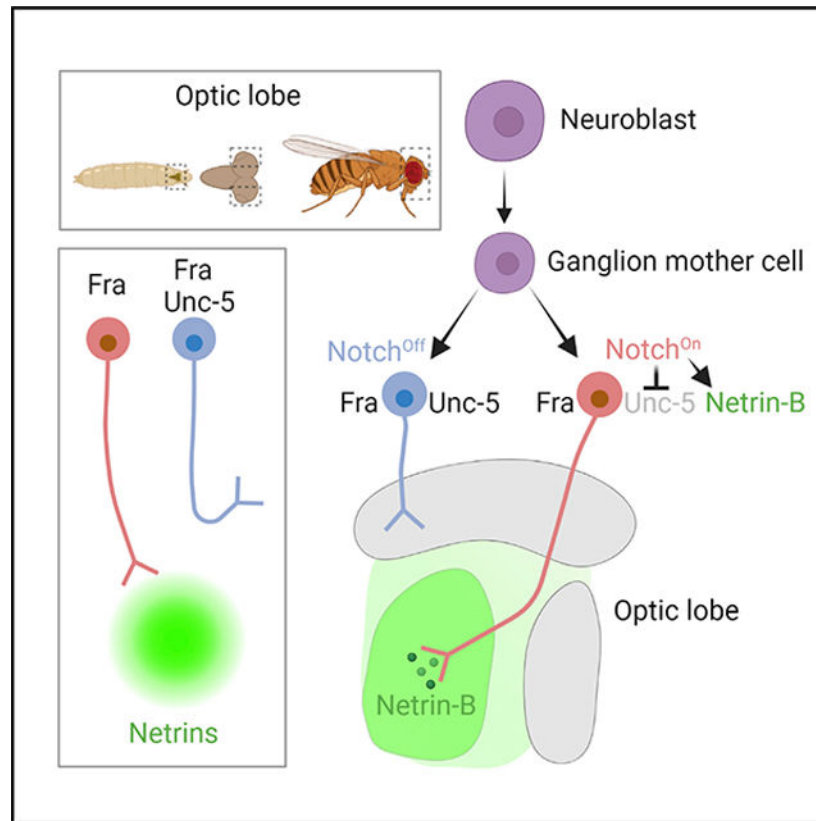
Conceptualization, Y.Z. and X.L.; investigation, Y.Z., S.L., and A.Z.D.; formal analysis and visualization, Y.Z.; writing – original draft, Y.Z. and X.L.; writing – review & editing, Y.Z., X.L., S.L., and A.Z.D.; funding acquisition, X.L.

#### DECLARATION OF INTERESTS

The authors declare no competing interests.

#### SUPPLEMENTAL INFORMATION

Supplemental information can be found online at <https://doi.org/10.1016/j.celrep.2023.112143>.



## INTRODUCTION

During neural development, a great diversity of neural types are specified and their axons navigate for a long distance to connect to their correct targets, which are critical steps in the development of neural circuits and assembly of neuropils. A large number of studies have focused on how neural diversity generation is controlled by neural fate specification programs including temporal and spatial patterning of neural progenitors and Notch-dependent binary fate choice between sister neurons.<sup>1-7</sup> Among them, Notch-dependent binary fate choice was first reported in the *Drosophila* nervous system, where the intermediate neural progenitor called ganglion mother cell (GMC) divides asymmetrically to generate two daughters of different fates, with one turning on Notch signaling and the other being Notch-off. All Notch-on neurons in a lineage constitute the Notch-on hemilineage, and all Notch-off neurons belong to the Notch-off hemilineage.<sup>8-11</sup> Generally, within a single lineage, Notch-on hemilineage neurons have distinct morphology and connections from the Notch-off hemilineage neurons, as illustrated in the *Drosophila* CNS, where Notch-on hemilineage neurons project to the motor neuropil, while Notch-off hemilineage neurons project to the sensory neuropil.<sup>12</sup> Recently, there is also evidence suggesting that Notch-dependent binary fate choice also contributes to neural diversity in vertebrates.<sup>13,14</sup>

In parallel, a wealth of studies over the past several decades have elaborated on the cellular machinery that shapes the neurons: extracellular guidance cues, such as Netrins, Slits, Semaphorins, Ephrins, certain morphogens, and growth factors, as well as cell-adhesion

molecules, act on their receptors or other cell-adhesion molecules on the cell surface; these cell-surface molecules are linked to intracellular signaling proteins, which then regulate the cytoskeleton dynamics.<sup>15–17</sup> For example, Netrins (NetA and NetB in *Drosophila*) are a family of conserved guidance cues, and Netrin binding induces homodimerization of DCC receptor (Frazzled or Fra in *Drosophila*), which leads to recruitment of downstream effectors and regulatory proteins, and finally causes an attractive response. In contrast, heterodimerization between DCC/Fra and receptor Uncoordinated locomotion 5 (Unc-5) leads to repulsion.<sup>18</sup>

However, studies linking the two fields are relatively lacking. It is not well understood how the upstream neural fate specification programs are “translated into” the highly organized neuropils by controlling coordinated axon targeting through regulation of downstream effectors such as guidance cues and cell surface molecules in different groups of neurons.

We address this question using the *Drosophila* visual system, which has been an excellent model system to study both neural fate specification and the mechanism of axon guidance. The adult *Drosophila* visual system is composed of the compound eye with ~800 ommatidia, and the optic lobe, which processes visual information and relays it to the central brain. The optic lobe consists of four neuropils, lamina, medulla, lobula, and lobula plate (Figure 1A), and each neuropil comprises ~800 units (columns or cartridges). The medulla, lobula, and lobula plate neuropils can be divided into 10 (M1–10), 6 (Lo1–6), and 4 (Lop1–4) layers, respectively. As the largest neuropil in the optic lobe, the medulla consists of ~40,000 neurons, classified into more than 80 neural types, belonging to several broad classes, including local neurons such as medulla intrinsic (Mi) neurons, distal medulla (Dm) neurons, and proximal medulla (Pm) neurons; and projection neurons such as transmedullary (Tm) neurons (connecting the medulla with the lobula) and transmedullary Y (TmY) neurons connecting the medulla with the lobula and lobula plate) and others.<sup>19–22</sup> These neurons are generated by medulla neuroblasts that are temporally and spatially patterned<sup>23–28</sup> (Figure 1B). Each medulla neuroblast divides asymmetrically multiple times to generate a series of GMCs, and each GMC divides once to give rise to two daughters of distinct fates, with one daughter turning on the Notch signaling and subsequently the transcription factor, Apterous (Ap), and the other daughter without Notch signaling.<sup>23</sup> Most Ap expressing medulla neurons (with the exception of Mi1 neurons, which are the Notch-on neurons generated in the first temporal stage) are visual projection neurons (Tm and TmY).<sup>20,29</sup> During development, there is a temporal gradient of Tm neuron targeting and lobula column assembly, with Tms from the most anterior medulla columns targeting the most proximal lobula columns first, followed by Tms from more posterior medulla columns targeting distal lobula columns later, thus forming the X-shaped inner optic chiasm (IOC)<sup>22</sup> (Figure 1A). However, it is not known which axon guidance pathway controls targeting of these projection neurons through the IOC, and how it is regulated by upstream neural specification programs.

Here, we report that the Netrin pathway controls Tm axon targeting to the lobula through the IOC, and the Netrin pathway components are regulated by Notch-dependent binary fate choice in medulla neurons. The expression of NetB and Unc-5 are activated and repressed by Notch signaling, respectively, in medulla neurons of the Notch-on hemilineage composed

of mostly Tm/TmY neurons that target the lobula. Repression of Unc-5 ensures that Tm neurons can target lobula, and after Tm axons from anterior early-born columns arrive at lobula, they secrete NetB and also contribute to NetB enrichment, which is essential for Tm axons from posterior later-born columns to join the IOC. Thus, Notch-dependent binary fate choice in medulla neurons contributes to the optic neuropil assembly through the Netrin axon guidance pathway.

## RESULTS

### Netrins are localized at the Tm targeting path and target neuropil

From the early third instar larval stage, medulla neuroblasts divide to generate diverse medulla neurons. Medulla neurons start to extend their axons shortly after birth, and at around 55% after puparium formation (APF), most of them have already arrived at their target layers, ready to form synapses and showing stimulus-independent neural activity.<sup>30</sup> To better understand the mechanism of medulla neuron targeting, we examined the expression patterns of known guidance cues, and found that Netrin-B (NetB) is highly enriched in the lobula neuropil and also present in the cleft between the medulla, lobula, and lobula plate at the third instar larval stage (Figures 1C and 1C1) and 24% APF (Figures 1D and 1D1). Netrin-A (NetA) is enriched at the boundaries around neuropils but not in the lobula at young pupal stage (Figures S1A and S1A1). Therefore, at the axon targeting stage, both NetA and NetB are present in the cleft between the medulla, lobula, and lobula plate, where Tm axons and other axons are actively targeting through the IOC, but only NetB is enriched in the lobula neuropil.

### Tm neurons express Fra but turn off Unc-5

Then, we examined the expression patterns of Netrin receptors in the third instar larval medulla cortex, where cell bodies of medulla neurons reside. We found that the two Netrin receptors, Fra and Unc-5, were expressed in the medulla cortex at the third instar larval stage. Fra is broadly expressed in the medulla cortex (Figures 1E–1E3), while Unc-5 is expressed in a subset of cells (Figures 1F–1F5). The GFP-tagged line and antibody staining of Fra were confirmed to show the same expression patterns (Figures S1C–S1D2), and the GFP-tagged line and *in situ* hybridization of Unc-5 were also confirmed to show the same expression patterns (Figures S1B–S1B2).

Previous studies found that axons expressing Fra but not Unc-5 are attracted to the Netrin source, while Unc-5 is required for the repulsive response away from the Netrin source.<sup>31,32</sup> Since NetB is enriched in the lobula neuropil at the beginning of the targeting stage, we speculated that medulla neurons that project to the lobula neuropil, i.e., Tm neurons (Figure 1A), should express the attractive receptor Fra, but not the repulsive receptor Unc-5. Most Tm neurons express the transcription factor Ap,<sup>20,29</sup> suggesting that they belong to the Notch-on hemilineage. Notch target gene Hey is transiently expressed in Notch-on medulla neurons,<sup>33</sup> and at 12% APF, Hey is already lost in the anterior early-born columns (Figure 1G1), while the expression of Ap is maintained throughout the lifetime in Notch-on neurons<sup>23</sup> (Figures S1E–S1E2 and 1H–1H2). Therefore, we co-stained Hey or Ap with Fra or Unc-5 at the third instar larval stage and pupal stages. We found Fra is expressed

broadly in medulla neurons including all Hey<sup>+</sup> neurons at third instar and 12% APF (Figures 1E–1E3 and 1G–1G2), suggesting that Tm neurons express Fra. We also found that Unc-5 expression in medulla neurons is dynamic: Unc-5 is highly expressed in young immature neurons (both Hey<sup>+</sup> and Hey<sup>–</sup>) located close to neuroblasts and GMCs (big arrows in Figures 1F–1F5); however, in older mature neurons undergoing axon targeting, Unc-5 is selectively downregulated in Hey-expressing neurons (small arrows in Figures 1F–1F5), with the exception of Mi1 which keeps expressing Unc-5 (small arrowhead in Figures S1F and 1F). We also noticed that a middle layer of neurons turn off Unc-5 expression regardless of whether they express Hey/Ap or not (big arrowhead in Figures 1F–1F2), and these neurons are likely to be generated in (and around) the Ey stage (one of the middle temporal stages during which neuroblasts express Ey) since some of them express Drifter (Figure S1G), which was shown to be expressed in the Ey stage progeny.<sup>23</sup> At 12% APF, when most Tm neurons are actively targeting their axons, all Ap<sup>+</sup> neurons have turned off Unc-5, and we observe a mutual exclusive expression pattern between Ap and Unc-5 (Figures 1H–1H2). Using cell-type-specific drivers, we confirmed that Tm neurons do not express Unc-5 during the axon targeting stage (examples shown in Figures S1H and S1I). In summary, we found that Fra is broadly expressed in both Notch-on and Notch-off medulla neurons, while Notch-on Tm neurons selectively turn off the repulsive receptor Unc-5 during their axon targeting.

### Netrin signaling regulates the formation of the inner chiasm

Since Fra but not Unc-5 is expressed in Tm neurons that target the NetB concentrated lobula neuropil, we next checked whether Netrin signaling was required for Tm axon targeting. We found that all Tm types examined lost the X-shaped structure in the cleft in *netAB* mutants (Figures 2B, 2D, and 2F). The X-shaped structure is IOC, formed by axons of posterior columns crossing all anterior axons before reaching the corresponding lobula columns (Figure 1A). The X-shaped IOC is essential for the maintenance of the retinotopic information. As a result of loss of the IOC, the relative orientation of lobula vs. medulla is changed from perpendicular to almost parallel. Therefore, Netrins are required for Tm targeting and the formation of IOC.

Next, we checked if Fra was the receptor responding to the Netrin cue in this process. By crossing *UAS-fraRNAi* with cell-type-specific drivers, we knocked down Fra specifically in different Tm neurons. We found that targeting of Tm axons through IOC was not affected by loss of Fra in individual neural types (Figures S2B and S2D). The knockdown efficiency of *UAS-fraRNAi* was confirmed by anti-Fra staining (Figures S2E–S2H). Thus, although Fra is expressed in diverse Tm neurons, knocking down Fra in individual Tm types did not affect the IOC.

The IOC is composed of crossing axon bundles, each of which consists of a number of different Tm axons. Therefore, we hypothesized that, within each bundle, Fra expressed on different Tm axons act redundantly to facilitate targeting of the whole bundle. To test this hypothesis, we needed to remove Fra in all Tm axons. We knocked down Fra using *SoxN-Gal4*, which is expressed only in the main medulla region neuroblasts and subsequently inherited in medulla neurons,<sup>28</sup> including all Tm neurons (Figure S2I). We found that IOC

formation was disrupted (Figures 2H and 2K) and some Tm axons seemingly cut through the lobula (arrows in Figures 2H and 2K), consistent with our hypothesis that Fra is required collectively in Tm axon bundles to target lobula through the IOC.

Since knocking down Fra in all medulla neurons might cause secondary effects, we designed a strategy to knock down Fra only in later-born posterior columns using temperature-sensitive Gal80 (*tubG180ts*) combined with *SoxN-Gal4*. A 24 h temperature shift to 29°C at early pupal stage only affected targeting of Tm axons in a number of later-born columns, while targeting of early-born columns is not affected (Figures 2I and 2L). These data demonstrate that the failure of IOC formation is a direct consequence of loss of Fra receptor in Tm bundles, but not a secondary effect.

To better view how Netrin signaling affects Tm joining the inner chiasm, we checked Tm targeting during development at 24% and 48% APF. We visualized the inner chiasm using Tm9. We knocked down Fra using *UAS-fraRNAi* driven by *ap-Gal4* (*ap>fraRNAi* hereafter), a Gal4 covering about half of the optic lobe neurons, including the majority of Tm and TmY neurons,<sup>20,29</sup> and checked the inner chiasm formation. In wild type, at 24% and 48% APF, the lobula neuropil was intact as labeled by phalloidin; all Tm9 neurons joined the inner chiasm and terminated at the superficial lobula layer (Figures 2M–2O). However, in *ap>fraRNAi* brains, some Tm9 axons do not turn to lobula but instead stop at the surface of the lobula plate; some Tm9 axons do not cross all of the adjacent anterior axons (Figures 2P–2R). Moreover, at 48% APF, Connectin labels a continuous lobula band in wild type (Figures 2N and 2O). In contrast, ectopic Connectin signals appear at the surface of the lobula plate where Tm9 axon terminals are mislocated in *ap>fraRNAi* (Figures 2Q and 2R). Consistently, lobula columns without Tm9 terminals are devoid of Connectin signals, creating the discontinuous Connectin band of lobula in *ap>fraRNAi* (Figures 2Q and 2R). To sum up, these data suggest that Netrin signaling is required for IOC formation. Without Netrin signaling, late-born axon bundles cannot cross all of the early-born axon bundles; instead, they stop at the surface of the lobula plate and continue the maturation locally, creating the disrupted IOC and the scattered lobula phenotype.

### **Fra expressed by medulla neurons contributes to NetB enrichment in the lobula**

Since the Netrin pathway is essential for Tm axon targeting to the lobula through the IOC, we next asked how NetB distribution was regulated. Previous studies found that Fra receptors expressed on axon terminals localize and enrich Netrin in embryonic CNS<sup>34</sup> and medulla layer M3.<sup>35</sup> We examined whether Fra also regulates NetB distribution in the lobula. First, we checked the distribution pattern of Fra and NetB in neuropils through development. At 24% APF, we found that Fra and NetB colocalize throughout the lobula neuropil (Figures 3A–3A3). At 48% APF, NetB was enriched at restricted domains (lobula layers 2 and 4–6), still colocalizing with Fra (Figures 3B–3B3). Next, we checked if NetB distribution was affected without Fra. We knocked down Fra by crossing *fraRNAi* with *ap-Gal4*. At 24% APF, NetB level in the lobula is reduced in *ap>fraRNAi* compared with control (Figures 3C–3D1 and 3H). The NetB signal in cell bodies is normal in *ap>fraRNAi*, indicating that NetB synthesis is not affected (Figures 3C–3D1). At 48% APF, in contrast to NetB enriching at restricted lobula domains in wild type, NetB level was significantly

reduced in *ap>fraRNAi* at the lobula (Figures 3F, 3F1, and 3I). Moreover, NetB enrichment at M3 is still continuous and the level is not affected in *ap>fraRNAi*. Because *ap-Gal4* also labels a subset of lobula and lobula plate neurons, we knocked down Fra using medulla neuron-specific *SoxN-Gal4*. Like *ap>fraRNAi*, the NetB level in lobula is significantly reduced in *SoxN>fraRNAi* compared with control (Figures 3G, 3G1, and 3I). Moreover, the NetB level at M3 is greatly reduced, consistent with targeting area Fra helps enrich NetB at M3 found in a previous study.<sup>35</sup> To sum up, these data indicated that Fra colocalized with NetB in neuropils, and that Fra expressed by medulla neurons (Tm/TmY neurons) contributes to NetB enrichment in lobula.

### Unc-5 may negatively regulate NetB enrichment

Since Fra is also broadly localized to lobula plate and medulla layers, which do not show NetB enrichment, we hypothesized that other molecules should also contribute to NetB distribution. The other known NetB receptor, Unc-5,<sup>32</sup> is a good candidate because it is highly expressed in the medulla and lobula plate neuropils where NetB is not enriched in early pupal stages (Figures 4A–4B3). At 48% APF, when neuropil layers start to be refined, NetB is enriched in medulla layer M3, and lobula layers Lo2 and Lo4–6, where Fra level is high and Unc-5 level is low (Figures S3A–S3A3). At 60% APF, NetB signals at lobula are all gone (Figures S3B–S3B3).

The largely complementary localization patterns of Unc-5 and NetB suggest a possibility that Unc-5 may negatively affect NetB enrichment. Therefore, we next examined whether loss of Unc-5 affects NetB distribution. In *unc-5* null mutants,<sup>36</sup> the NetB synthesis in the cell bodies at the medulla cortex was the same as wild type (Figures 4C–4D1). In contrast to the specific lobula enrichment of NetB in wild type (Figures 4C and 4C1), in *unc-5* mutant at 24% APF, NetB is also enriched in the lobula plate and medulla neuropils (Figures 4D and 4D1). At 48% APF in *unc-5* mutant, NetB is no longer enriched in specific layers of lobula; instead, high-intensity dotted signals of NetB are observed throughout the optic lobe, especially in the cleft between neuropils (Figures 4F and 4F1). Moreover, the NetB signal at the M3 layer was also smearing in *unc-5* mutants, indicating that loss of Unc-5 affected NetB distribution throughout the optic lobe. Consistently, the IOC was disrupted in *unc-5* mutants (Figure S3D). Therefore, our results suggest that loss of Unc-5 causes NetB to spread abnormally, which affects Tm targeting non-cell autonomously.

Next, we checked whether ectopically expressing Unc-5 would affect NetB enrichment. We overexpressed Unc-5 by crossing *UAS-HA-unc-5* with *ap-Gal4* and found that the NetB level at M3 was significantly reduced (Figures 4H and 4H1). In addition, the structure of the lobula complex was totally damaged; lobula and lobula plate can be barely distinguished, and no enrichment of NetB was observed in any part of the lobula complex (Figures 4H and 4H1). Taken together, although there is a possibility that the abnormal projections of Fra-positive neurons in *unc-5* mutants may indirectly affect the ligand distribution, our results suggest that the absence of Unc-5 in Ap-expressing neurons is necessary for NetB enrichment in the lobula.

### Notch signaling plays a role in downregulation of Unc-5 expression

Next, we examined how Unc-5 expression in medulla neurons is regulated. Since Fra is ubiquitously expressed in medulla neurons, the response to Netrin depends on the presence or absence of Unc-5. Our data showed that Unc-5 expression was dynamically regulated in Tm neurons: activated in young immature neurons while repressed in mature Notch-on neurons undergoing axon targeting. By overexpressing Unc-5 with cell-type-specific drivers, we found that Tm axons were stalled at the lobula surface or mistargeted to the lobula plate (Figures 5C and 5D compared with control Figures 5A and 5B). Therefore, turning off the repulsive Unc-5 is critical for properly targeting of Tm axons to lobula.

Since Tm neurons cannot express Unc-5 during axon targeting, and most Tm neurons are Notch-on, we checked if Notch signaling is required to inhibit Unc-5 expression in Tm neurons. We hypothesized that loss of Notch signaling should result in ectopic activation of Unc-5. Using *in situ* hybridization, we found that, in wild type, Unc-5 mRNA is enriched in late-stage neuroblasts, young neurons located close to surface, a subset of early-born neurons including Mi1 and Runt+ neurons (Runt+ neurons are Notch-off neurons generated in the early temporal stage), and a subset of late-born neurons (Figures 5E–5E3), consistent with the Unc-5-GFP expression pattern (Figures S1B–S1B2). In contrast, ectopic Unc-5 mRNA signals can be observed in *Su(H)* mutant MARCM clones (Figures 5F–5G3 and S4A–S4A3). In clones spanning Runt neurons, we noticed that an extra number of Runt+ neurons were compacted together in *Su(H)* mutant MARCM clones, and Unc-5 signals were also expanded (Figures 5F–5F3), suggesting that, in these mutant clones, Notch-on neurons were transformed into their Notch-off twin sisters and started to express Unc-5. In neurons born from late temporal stages, we also observed compacted Unc-5 signals in *Su(H)* mutant MARCM clones in contrast to the scattered signals in surrounding wild-type regions (Figures 5G1–5G3 and S4A–S4A3). However, not all mutant clones showed ectopic Unc-5 signals, and we reasoned that, in those regions, other factors or mechanisms are present to repress Unc-5 expression, consistent with our observation that, in wild-type medulla, a layer of middle-stage-born neurons turn off Unc-5 expression regardless of whether they express Ap or not. Therefore, the regulation of Unc-5 expression may involve a lot of different mechanisms, but among them Notch signaling also play a role in inhibiting the expression of Unc-5 in Notch-on neurons, which is necessary for their targeting to the NetB-enriched lobula.

### Notch signaling is required to activate NetB expression

We next examined which neurons are the source of NetB and found that three groups of lobula-targeting neurons with cell bodies located in the lobula, lobula plate, and medulla cortex, respectively, express NetB (Figure S4B), suggesting that they may all contribute to the NetB pool in the lobula. To connect NetB expression with the upstream regulator, we analyzed published scRNA-seq data of early pupal optic lobe neurons<sup>29</sup> and found that the top transcription factor whose expression correlates with NetB is Ap (Figure S4C). Ap is expressed in all Notch-on medulla neurons, and Ap expression is lost when Notch signaling is lost in *Su(H)* mutant clones.<sup>23</sup> We checked if NetB was expressed by Notch-on medulla neurons and found that indeed all NetB-expressing cells in the medulla cortex are also labeled by Ap-lacZ (Figures 6A–6A2), although not all Notch-on neurons express NetB



(Figures S4D–S4D3). Next, we examined whether Ap regulated NetB expression. However, NetB expression was not affected in ap mutants (Figures S4E and S4E1). Then, we checked if NetB expression was regulated by Notch signaling and found that NetB staining was lost in *Su(H)* mutant MARCM clones (Figures 6C–6C2). Consistently, knocking down Su(H) by *elav-Gal4>Su(H) RNAi* abolished NetB expression in the medulla cortex (Figures S4G and S4G1). We also examined if Notch signaling was sufficient to activate NetB expression. First, we tried to activate Notch signaling by removing Numb, which inhibits Notch activity.<sup>8</sup> However, we found predominantly ectopic neuroblasts in the mutant clones, prohibiting further analysis of NetB expression in neurons (Figures S4H–S4H2). Then, we activated Notch signaling in subsets of neurons by overexpressing Notch intracellular domain (NICD) with *pros-gal4*, which starts expression in GMCs and is inherited by progenies in combination with tubGal80ts and temperature shift. We used Hey as a reporter for Notch activity and examined NetB expression at 24% APF when NetB is strongly expressed at the medulla cortex. In control, we observed Hey expression only in newly born neurons since Hey disappeared in old neurons (Figure S4I). In *pros-gal4* driving *NICD* brains, we found Hey expression appeared in some old neurons, suggesting that Notch signaling was activated in these neurons by overexpressing NICD. However, not all of these Notch-on cells express NetB (Figures S4J–S4J2), suggesting that Notch signaling is not sufficient to activate NetB expression. Taken together with the expression pattern that not all Notch-on neurons express NetB, our data suggest that, in addition to Notch signaling, other factors should also be required to activate NetB expression.

In summary, these data suggest that Notch signaling is necessary but not sufficient to activate NetB expression in medulla neurons.

### **Coordinate repression of Unc-5 and activation of NetB by Notch signaling regulate Tm axon targeting**

We showed that Notch signaling is involved in repression of Unc-5 expression in neurons targeting lobula, and at the same time required for their NetB expression. Does this coordinate regulation have a functional significance? We reasoned that Tm neurons from anterior medulla columns arrive at the lobula earlier and contribute to the NetB pool, which may help Tm targeting from posterior columns that arrive later. To test whether NetB derived from medulla neurons affects Tm targeting in later-born posterior columns, we knocked down NetB only in medulla neurons using *SoxN-Gal4>netBRNAi*, and indeed we observed disrupted IOC formation and mistargeting to the lobula plate from Tm neurons in posterior columns (Figure 6E). Taken together, we showed that Notch signaling is required to turn off Unc-5 in Tm neurons so that they will target lobula, and at the same time Notch signaling is required to turn on NetB expression in Tm neurons, and medulla-derived NetB is required for the correct targeting of Tm neurons from later-born columns. Therefore, our results suggest that the Notch-dependent binary fate choice coordinately regulates the ligand and receptor of the Netrin guidance pathway and contributes to the correct assembly of the neuropils (Figure 7).

## DISCUSSION

During nervous system development, neural diversity is generated through integration of temporal patterning, spatial patterning, and Notch-dependent binary fate choice between sister neurons. How these upstream neural specification programs are translated into highly organized neuropils is not well understood. In this work, using the *Drosophila* visual system as an example, we demonstrate that Notch signaling regulates the expression of Netrin pathway components in Notch-on hemilineage neurons, and that the Netrin pathway controls targeting of visual projection neurons (Tm) to the higher order neuropil (lobula). Notch signaling is required to repress *Unc-5* expression in Tm neurons (Figure 7A). The absence of *Unc-5* is essential for Tm neurons to target lobula, and also required for Tm neurons to further enrich NetB in lobula using the Fra receptor. Furthermore, Notch signaling is required to activate NetB expression in Tm neurons, and medulla-derived NetB has an essential role in promoting targeting of Tm axons from later-born medulla columns to lobula through the IOC (Figure 7B). Here, we discuss the regulation of NetB distribution and the regulation of Netrin pathway components by Notch signaling and possibly other factors.

### Fra and possibly *Unc-5* regulate NetB enrichment in the optic lobe

Previous studies found that, in other neuropils, Fra captures NetB to enrich them locally.<sup>34,35</sup> Here, we also found that Fra is colocalized with NetB in lobula neuropil layers. Without Fra expressed in medulla projection neurons, NetB enrichment at lobula is greatly diminished. However, since Fra also guides the targeting of Tm neurons to lobula and Tm neurons are also part of the Netrin source, it is possible that both mechanisms contribute to the diminished NetB in the lobula.

Although Fra is required for NetB enrichment, not all Fra are colocalized with NetB in the optic lobe. Furthermore, we found that *Unc-5* may be a negative regulator of NetB enrichment. In *unc-5* mutants, NetB spreads to lobula plate and medulla. Moreover, overexpression of *Unc-5* results in disrupted NetB distribution. However, how *Unc-5* regulates NetB distribution requires future investigation. *Unc-5* may affect NetB distribution directly or indirectly by affecting the guidance of specific neurons, which affect NetB distribution.

### Notch is involved in the regulation of *Unc-5* expression

Since mis-expressing *Unc-5* in Tm neurons results in their repulsion to the lobula plate, *Unc-5* expression should be strictly inhibited in Tm neurons during axon targeting. We found that *Unc-5* expression was activated ectopically without Notch signaling, likely in most Tm neurons. However, the regulation of *Unc-5* expression in medulla neurons is far more complex and may involve multiple factors/mechanisms. First, besides Tm neurons, Notch-on hemilineage also includes Mi1 neurons, which terminate at the proximal medulla neuropil, and they do keep expressing *Unc-5*. Therefore, Notch signaling does not inhibit *Unc-5* expression in all Notch-on neurons, and in these exceptions, like Mi1 neurons, other factors, such as TTF or neuronal-specific transcription factors, might override the inhibition of *Unc-5* expression by Notch signaling. Consistent with this hypothesis, loss of Hth or Bsh transforms Mi1 into a Tm-type neuron.<sup>37,38</sup> Second, there should be other

factors or mechanisms that repress *Unc-5* expression in medulla neurons. We observed a middle layer of neurons (likely born in and around the Ey temporal stage) that turn off *Unc-5* regardless of their Notch status. Although most Tm and TmY neurons belong to the Notch-on hemilineage, there are a few exceptions; for example, scRNA-seq data showed that Tm5c, Tm29, and a few TmY neuron types do not express *Ap*.<sup>29,39–42</sup> Among them, Tm29, TmY5a, and TmY14 are shown to express *Knot* (*Kn*),<sup>29,39–42</sup> and are thus generated from the Notch-off hemilineage in the Ey stage<sup>28</sup> (corresponding to the middle-layer gap in *unc-5* expression). Thus, these neurons likely turn off *Unc-5* by a different mechanism independent of Notch signaling. It will be interesting to examine whether the TTF(s) or neuronal transcription factors such as *Kn* are involved. Third, while *Unc-5* is expressed in most young immature neurons, it is turned off later in Notch-on neurons, suggesting that a later-acting factor that is specifically activated in the Notch-on hemilineage is required to turn off *Unc-5* expression.

### **Notch-dependent regulation of Netrin pathway components contributes to the neuropil assembly**

In addition to repression of *Unc-5*, we also showed that Notch signaling is required to activate *NetB* expression in Notch-on medulla neurons. Thus, our results suggest that Notch-dependent binary fate choice ensures that lobula-targeting neurons will turn on *NetB* expression and provide more *NetB* to the lobula *NetB* pool (Figures 7A and 7B). Tm axons from later-born posterior medulla columns may require a higher concentration of *NetB* to target lobula, because of the longer distance they need to migrate. Consistently, when we knocked down medulla-derived *NetB* using *SoxN-Gal4*, Tm axons from posterior columns showed disrupted IOC formation.

Taken together, our results suggest that, in the Notch-on hemilineage neurons, Notch signaling is required to repress the repulsive receptor *Unc-5* and also to activate the expression of *NetB*, which ensures that projection neurons targeting lobula can further enrich *NetB* with their *Fra* receptors as well as secrete more *NetB*. This positive feedback mechanism is required for the correct formation of IOC through which visual project neurons connect to their target neuropil. Thus, Notch-dependent binary fate choice in medulla neurons coordinately regulates the expression of an axon guidance cue and its receptors, which is required for the correct assembly of neuropils (Figures 7A and 7B).

### **Limitations of the study**

We demonstrated that Notch signaling is required to regulate Netrin pathway components. However, it is not known whether this regulation is direct or indirect. In addition, the regulation of Netrin pathway components is complex, and should involve integration of Notch signaling with other factors such as temporal factors and spatial factors.

## **STAR★METHODS**

### **RESOURCE AVAILABILITY**

**Lead contact**—Further information and requests for resources and reagents should be directed to and will be fulfilled by the lead contact, Xin Li (lixin@illinois.edu).

**Materials availability**—This study did not generate new unique reagents.

#### Data and code availability

- This paper analyzes existing, publicly available data. These accession numbers for the datasets are listed in the key resources table. The published scRNA-seq data of early pupal optic lobe cells (early dataset, 0h–24h APF) were downloaded from NCBI GEO: GSE156455. Microscopy data reported in this paper will be shared by the lead contact upon request.
- The codes used for analyzing the published scRNA-seq data of early pupal optic lobe cells is included as Data S1.
- Any additional information required to reanalyze the data reported in this paper is available from the lead contact upon request.

### EXPERIMENTAL MODEL AND SUBJECT DETAILS

**Fly stocks**—Fly stocks were maintained in standard medium at 25°C except for RNAi experiments, for which crosses were grown at 29°C. The following stocks/crosses were used for expression analyses: *netA netB<sup>myc</sup>* (from B. J. Dickson); *fra-GFP* (BL 59835); *unc-5-GFP* (BL 64547); *UAS-myr-mRFP* (BL7118); *UAS-cd8GFP*; *27b-Gal4 (Tm1-Gal4)<sup>20</sup>*; *Tm9-Gal4* (BL 48050); *Tm3-Gal4* (BL48569) for adult labeling; *Tm3-Gal4* (BL76324) for larva labeling; *Tm4-Gal4* (BL49922); *Tm3-lexA* (BL52459), *lexopTdTomato*; *ap-lacZ*.<sup>43</sup> The following stocks were used for loss of function mutants: *netA netB /FM7* (from B. J. Dickson); *Unc-5<sup>8</sup>/CyO* (from G. J. Bashaw), *FRT40 Su(H)<sup>D47</sup>/CyO* and *numb<sup>15</sup> FRT40A/CyO* (both are gifts from F. Schweisguth). The following stocks/crosses were used in RNAi experiments: *UAS-fraRNAi* (BL 40826); *UAS-netB-RNAi* (BL25861); *UAS-Su(H)-RNAi* (VDRC 103597), *UAS-unc-5RNAi* (BL33756); *tll-Gal4* (GMR31H09, BL 49694); *elav-Gal4*; *UAS-Dcr2* (BL 25750); *ap-Gal4<sup>43</sup>*; *SoxN-Gal4* (GMR41H10Gal4); *Tm9-lexA* (BL54982). The following stocks were used with gain-of-function analyses: *UAS-HA-Unc-5* (from G. J. Bashaw).

### METHOD DETAILS

**Immunostaining and antibodies**—Wandering 3<sup>rd</sup> instar larvae were picked for larval stage immunostaining. White pupae were growing to certain age either in a Petri dish layered with hydrated filter paper when growing at 25°C or in a vial of food at 29°C. The pupal stage lasts about 100 hr when growing at 25°C and about 78 hr at 29°C. As a result, 24% APF means growing white pupae for 24 hours at 25°C and about 19 hours at 29°C. Immunostaining was done as described previously<sup>23</sup> with a few modifications. Brains were dissected in phosphate-buffered saline (PBS), fixed for 30 min for the 3<sup>rd</sup> instar larvae, 40 min for pupae and adult at room temperature in 4% paraformaldehyde in PBS, washed in PBS containing 0.3% Triton X-100. Brains were then incubated in primary antibody solution at 4°C overnight, washed three times with PBST, incubated in secondary antibody solution at room temperature for 3 hours, washed three times with PBST and three times with PBS and mounted in Slowfade.

The following primary antibodies were used: rabbit anti-NetB (from B.Altenein, 1:100), rabbit anti-NetA (from B.Altenein, 1:100), sheep anti-GFP (AbD Serotec: 4745–1051, 1:500), Phalloidin-iFluor 405 (Abcam: ab176752, 1:1000), rabbit anti-RFP (Abcam: ab62341, 1:1000), rabbit anti-fra (from Y.N. Jan, 1:400), guinea pig anti-Hey (from C. Delidakis, 1:1000), rat anti-Dfr (from M. Sato, 1:100), mouse anti-Cut (DSHB:2B10, 1:10), chicken anti-lacZ (Abcam: ab9361, 1:800), guinea-pig anti-Runt (from C. Desplan, 1:500), mouse anti-Myc (DSHB: 9E10, 1:10), rat anti-DN-cadherin (DSHB: DN-Ex#8, 1:50), mouse anti-Connectin (DSHB:C1.427, 1:10).

Secondary antibodies were from Jackson or Invitrogen. Images are acquired using a Zeiss Confocal Microscope. Figures are assembled using Photoshop and Illustrator.

**Generate MARCM clones**—To generate wild-type, *Su(H)* mutant MARCM clones, or numb mutant MARCM clones, flies of *y,w,hsFLP,UAS-CD8::GFP; FRT40A, tub-Gal80; tub-Gal4/TM6B* were crossed with *FRT40A*, or *FRT40A, Su(H)<sup>47</sup>/CyO*, or *FRT40A, numb15/CyO* flies (gifts from F. Schweisguth). To induce mutant clones, the progenies were heat-shocked at 37°C for 1 hour at early larval stage and dissected at adult or 30% APF.

**Generate *ap* mutant clones**—For *ap* mutants, flies of *Mi{FlpStop}apMI01996-FlpStop.ND/CyO* (BL67675) were crossed with *ap-Gal4/CyO* (*ap-Gal4* is a homozygous lethal insertion in *ap* locus). To induce mutant clones, the progenies were heat-shocked at 37°C at early larval stage and dissected at 30% APF.<sup>44</sup> Cells expressing RFP are *ap-FlpStop* mutation over *ap-Gal4* mutation.

**Experiments using temperature sensitive Gal80**—To knock down Fra specifically in late-born columns, we crossed *tubG180ts/Cyo; SoxN-Gal4 with UAS-fraRNAi*. The flies were raised at 25°C until the early pupal stage. Then, they were shifted to 29°C for 24 hrs and transferred back to 25°C until eclosion.

To activate Notch signaling in subset of GMCs and neurons, we crossed *tubG180ts/Cyo; pros-Gal4 with UAS-NICD*. The flies were raised at 25°C until the early 3rd instar larval stage. Then, they were shifted to 29°C for 48 hr and transferred back to 25°C until 24% APF when they were dissected.

**In situ hybridization**—*In situ* hybridization for Unc-5 was used to detect its mRNA following a published protocol<sup>45</sup> except for the treatment step with NaBH<sub>4</sub>. Probes were designed in the online Stellaris Designer using the transcript sequence of common exons for Unc-5 isoforms. Forty-eight 20 nt-long probes were ordered from Biosearch Technologies. Probes were diluted to 0.25 μM in the final staining.

## QUANTIFICATION AND STATISTICAL ANALYSIS

For the targeting defect: at least five brains were imaged, and in each brain numbers of axon terminals from at least three different focal planes were counted. For NetB level analysis, images were taken with the same confocal parameters for control and test groups. Histogram tool from photoshop was used and median values from regions of interest were calculated.

## Supplementary Material

Refer to Web version on PubMed Central for supplementary material.

## ACKNOWLEDGMENTS

We thank the fly community, especially Greg J. Bashaw, Benjamin Altenhein, Yuh Nung Jan, C. Delidakis, Barry J. Dickson, and Claude Desplan for generous gifts of antibodies and fly stocks. We thank the Bloomington Drosophila Stock Center, the Vienna Drosophila RNAi Center, the Developmental Studies Hybridoma Bank, and TriP at Harvard Medical School (NIH/NIGMS R01-GM084947) for fly stocks and reagents. We thank Filipe Pinto-Teixeira, Isabel Holguera, and Neset Ozel for helpful discussions. This work was supported by the National Institutes of Health (grant nos. R01 EY026965–01A1 and R01 EY026965–06A0 to X.L.).

## REFERENCES

- Guillemot F (2007). Spatial and temporal specification of neural fates by transcription factor codes. *Development* 134, 3771–3780. 10.1242/DEV.006379. [PubMed: 17898002]
- Lin S, and Lee T (2012). Generating neuronal diversity in the Drosophila central nervous system. *Dev. Dyn.* 241, 57–68. 10.1002/DVDY.22739. [PubMed: 21932323]
- Allan DW, and Thor S (2015). Transcriptional selectors, masters, and combinatorial codes: regulatory principles of neural subtype specification. *Wiley Interdiscip. Rev. Dev. Biol.* 4, 505–528. 10.1002/WDEV.191. [PubMed: 25855098]
- Holguera I, and Desplan C (2018). Neuronal specification in space and time. *Science* 362, 176–180. 10.1126/SCIENCE.AAS9435. [PubMed: 30309944]
- Doe CQ (2017). Temporal patterning in the Drosophila CNS. *Annu. Rev. Cell Dev. Biol.* 33, 219–240. 10.1146/ANNUREV-CELLBIO-111315-125210. [PubMed: 28992439]
- Sagner A, and Briscoe J (2019). Establishing neuronal diversity in the spinal cord: a time and a place. *Development* 146. 10.1242/DEV.182154.
- Azzarelli R, Hardwick LJA, and Philpott A (2015). Emergence of neuronal diversity from patterning of telencephalic progenitors. *Wiley Interdiscip. Rev. Dev. Biol.* 4, 197–214. 10.1002/wdev.174. [PubMed: 25619507]
- Spana EP, and Doe CQ (1996). Numb antagonizes Notch signaling to specify sibling neuron cell fates. *Neuron* 17, 21–26. 10.1016/s0896-6273(00)80277-9. [PubMed: 8755475]
- Skeath JB, and Doe CQ (1998). Sanpodo and Notch act in opposition to Numb to distinguish sibling neuron fates in the Drosophila CNS. *Development* 125. 10.1242/dev.125.10.1857.
- Truman JW, Moats W, Altman J, Marin EC, and Williams DW (2010). Role of Notch signaling in establishing the hemilineages of secondary neurons in Drosophila melanogaster. *Development* 137, 53–61. 10.1242/dev.041749. [PubMed: 20023160]
- Lee YJ, Yang CP, Miyares RL, Huang YF, He Y, Ren Q, Chen HM, Kawase T, Ito M, Otsuna H, et al. (2020). Conservation and divergence of related neuronal lineages in the drosophila central brain. *Elife* 9, e53518. 10.7554/eLife.53518. [PubMed: 32255422]
- Mark B, Lai SL, Zarin AA, Manning L, Pollington HQ, Litwin-Kumar A, Cardona A, Truman JW, and Doe CQ (2021). A developmental framework linking neurogenesis and circuit formation in the drosophila CNS. *Elife* 10, e67510. 10.7554/eLife.67510. [PubMed: 33973523]
- Peng CY, Yajima H, Burns CE, Zon LI, Sisodia SS, Pfaff SL, and Sharma K (2007). Notch and MAML signaling drives Scl-dependent interneuron diversity in the spinal cord. *Neuron* 53, 813–827. 10.1016/j.neuron.2007.02.019. [PubMed: 17359917]
- Engerer P, Petridou E, Williams PR, Suzuki SC, Yoshimatsu T, Portugues R, Mischak T, and Godinho L (2021). Notch-mediated re-specification of neuronal identity during central nervous system development. *Curr. Biol.* 31, 4870–4878.e5. 10.1016/j.cub.2021.08.049. [PubMed: 34534440]
- Dorskind JM, and Kolodkin AL (2021). Revisiting and refining roles of neural guidance cues in circuit assembly. *Curr. Opin. Neurobiol.* 66, 10–21. 10.1016/J.CONB.2020.07.005. [PubMed: 32823181]

16. Kolodkin AL, and Tessier-Lavigne M (2011). Mechanisms and molecules of neuronal wiring: a primer. *Cold Spring Harb. Perspect. Biol.* 3, a001727. 10.1101/CSHPERSPECT.A001727. [PubMed: 21123392]
17. Stoeckli ET (2018). Understanding axon guidance: are we nearly there yet? *Development* 145, dev151415. 10.1242/DEV.151415. [PubMed: 29759980]
18. Boyer NP, and Gupton SL (2018). Revisiting netrin-1: one who guides (axons). *Front. Cell. Neurosci.* 12, 221. 10.3389/FNCEL.2018.00221/BIBTEX. [PubMed: 30108487]
19. Fischbach KF, and Dittrich APM (1989). The optic lobe of *Drosophila melanogaster*. I. A Golgi analysis of wild-type structure. *Cell Tissue Res.* 258, 441–475. 10.1007/BF00218858.
20. Morante J, and Desplan C (2008). The color-vision circuit in the medulla of *Drosophila*. *Curr. Biol.* 18, 553–565. 10.1016/J.CUB.2008.02.075. [PubMed: 18403201]
21. Nern A, Pfeiffer BD, and Rubin GM (2015). Optimized tools for multicolor stochastic labeling reveal diverse stereotyped cell arrangements in the fly visual system. *Proc. Natl. Acad. Sci. USA* 112, E2967–E2976. 10.1073/PNAS.1506763112. [PubMed: 25964354]
22. Ngo KT, Andrade I, and Hartenstein V (2017). Spatio-temporal pattern of neuronal differentiation in the *Drosophila* visual system: a user's guide to the dynamic morphology of the developing optic lobe. *Dev. Biol.* 428, 1–24. 10.1016/J.YDBIO.2017.05.008. [PubMed: 28533086]
23. Li X, Erclik T, Bertet C, Chen Z, Voutev R, Venkatesh S, Morante J, Celik A, and Desplan C (2013). Temporal patterning of *Drosophila* medulla neuroblasts controls neural fates. *Nature* 498, 456–462. 10.1038/nature12319. [PubMed: 23783517]
24. Suzuki T, Kaido M, Takayama R, and Sato M (2013). A temporal mechanism that produces neuronal diversity in the *Drosophila* visual center. *Dev. Biol.* 380, 12–24. 10.1016/J.YDBIO.2013.05.002. [PubMed: 23665475]
25. Erclik T, Li X, Courgeon M, Bertet C, Chen Z, Baumert R, Ng J, Koo C, Arain U, Behnia R, et al. (2017). Integration of temporal and spatial patterning generates neural diversity. *Nature* 541, 365–370. 10.1038/nature20794. [PubMed: 28077877]
26. Konstantinides N, Holguera I, Rossi AM, Escobar A, Dudragne L, Chen YC, Tran TN, Martínez Jaimes AM, Özel MN, Simon F, et al. (2022). A complete temporal transcription factor series in the fly visual system. *Nature* 604, 316–322. 10.1038/s41586-022-04564-w. [PubMed: 35388222]
27. Tang JLY, Hakes AE, Krautz R, Suzuki T, Contreras EG, Fox PM, and Brand AH (2022). NanoDam identifies homeobrain (ARX) and scarecrow (NKX2.1) as conserved temporal factors in the *Drosophila* central brain and visual system. *Dev. Cell* 57, 1193–1207.e7. 10.1016/J.DEVCEL.2022.04.008. [PubMed: 35483359]
28. Zhu H, Zhao SD, Ray A, Zhang Y, and Li X (2022). A comprehensive temporal patterning gene network in *Drosophila* medulla neuroblasts revealed by single-cell RNA sequencing. *Nat. Commun.* 13, 1247. 10.1038/s41467-022-28915-3. [PubMed: 35273186]
29. Kurmangaliyev YZ, Yoo J, Valdes-Aleman J, Sanfilippo P, and Zipursky SL (2020). Transcriptional programs of circuit assembly in the *Drosophila* visual system. *Neuron* 108, 1045–1057.e6. 10.1016/J.NEURON.2020.10.006. [PubMed: 33125872]
30. Akin O, Bajar BT, Keles MF, Frye MA, and Zipursky SL (2019). Cell-type-specific patterned stimulus-independent neuronal activity in the *Drosophila* visual system during synapse formation. *Neuron* 101, 894–904.e5. 10.1016/J.NEURON.2019.01.008. [PubMed: 30711355]
31. Kolodziej PA, Timpe LC, Mitchell KJ, Fried SR, Goodman CS, Jan LY, and Jan YN (1996). Frazzled encodes a *Drosophila* member of the DCC immunoglobulin subfamily and is required for CNS and motor axon guidance. *Cell* 87, 197–204. 10.1016/S0092-8674(00)81338-0. [PubMed: 8861904]
32. Keleman K, and Dickson BJ (2001). Short- and long-range repulsion by the *Drosophila* Unc5 netrin receptor. *Neuron* 32, 605–617. 10.1016/S0896-6273(01)00505-0. [PubMed: 11719202]
33. Bertet C, Li X, Erclik T, Cavey M, Wells B, and Desplan C (2014). Temporal patterning of neuroblasts controls notch-mediated cell survival through regulation of hid or reaper. *Cell* 158, 1173–1186. 10.1016/j.cell.2014.07.045. [PubMed: 25171415]
34. Hiramoto M, Hiromi Y, Giniger E, and Hotta Y (2000). The *Drosophila* netrin receptor Frazzled guides axons by controlling netrin distribution. *Nature* 406, 886–889. 10.1038/35022571. [PubMed: 10972289]

35. Timofeev K, Joly W, Hadjieconomou D, and Salecker I (2012). Localized Netrins act as positional cues to control layer-specific targeting of photoreceptor axons in *Drosophila*. *Neuron* 75, 80–93. 10.1016/J.NEURON.2012.04.037. [PubMed: 22794263]
36. Labrador JP, O’Keefe D, Yoshikawa S, McKinnon RD, Thomas JB, and Bashaw GJ (2005). The homeobox transcription factor even-skipped regulates netrin-receptor expression to control dorsal motoraxon projections in *Drosophila*. *Curr. Biol.* 15, 1413–1419. 10.1016/j.cub.2005.06.058. [PubMed: 16085495]
37. Hasegawa E, Kaido M, Takayama R, and Sato M (2013). Brain-specific-homeobox is required for the specification of neuronal types in the *Drosophila* optic lobe. *Dev. Biol.* 377, 90–99. 10.1016/j.ydbio.2013.02.012. [PubMed: 23454478]
38. Hasegawa E, Kitada Y, Kaido M, Takayama R, Awasaki T, Tabata T, and Sato M (2011). Concentric zones, cell migration and neuronal circuits in the *Drosophila* visual center. *Development* 138, 983–993. 10.1242/dev.058370. [PubMed: 21303851]
39. Konstantinides N, Kapuralin K, Fadil C, Barboza L, Satija R, and Desplan C (2018). Phenotypic convergence: distinct transcription factors regulate common terminal features. *Cell* 174, 622–635.e13. 10.1016/J.CELL.2018.05.021. [PubMed: 29909983]
40. Davis FP, Nern A, Picard S, Reiser MB, Rubin GM, Eddy SR, and Henry GL (2020). A genetic, genomic, and computational resource for exploring neural circuit function. *Elife* 9, e50901. 10.7554/ELIFE.50901. [PubMed: 31939737]
41. Kurmangaliyev YZ, Yoo J, Locascio SA, and Zipursky SL (2019). Modular transcriptional programs separately define axon and dendrite connectivity. *Elife* 8, e50822. 10.7554/ELIFE.50822. [PubMed: 31687928]
42. Özel MN, Simon F, Jafari S, Holguera I, Chen YC, Benhra N, El-Danaf RN, Kapuralin K, Malin JAKonstantinides N, and Desplan C (2021). Neuronal diversity and convergence in a visual system developmental atlas. *Nature* 589, 88–95. 10.1038/s41586-020-2879-3. [PubMed: 33149298]
43. Cohen B, McGuffin ME, Pfeifle C, Segal D, Cohen SM, and Stephen M,C. (1992). *apterous*, a gene required for imaginal disc development in *Drosophila* encodes a member of the LIM family of developmental regulatory proteins. *Genes Dev.* 6, 715–729. 10.1101/GAD.6.5.715. [PubMed: 1349545]
44. Fisher YE, Yang HH, Isaacman-Beck J, Xie M, Gohl DM, and Clandinin TR (2017). *FlpStop*, a tool for conditional gene control in *Drosophila*. *Elife* 6, e22279. 10.7554/ELIFE.22279. [PubMed: 28211790]
45. Long X, Colonell J, Wong AM, Singer RH, and Lionnet T (2017). Quantitative mRNA imaging throughout the entire *Drosophila* brain. *Nat. Methods* 14, 703–706. 10.1038/nmeth.4309. [PubMed: 28581495]



**Highlights**

- Notch signaling is required to regulate the expression of Netrin pathway components
- Netrin pathway is required in optic lobe assembly and targeting of projection neurons
- Netrin distribution in the optic lobe is regulated by its receptors, Fra and Unc-5
- Medulla-derived Netrin promotes targeting of projection axons from later-born columns

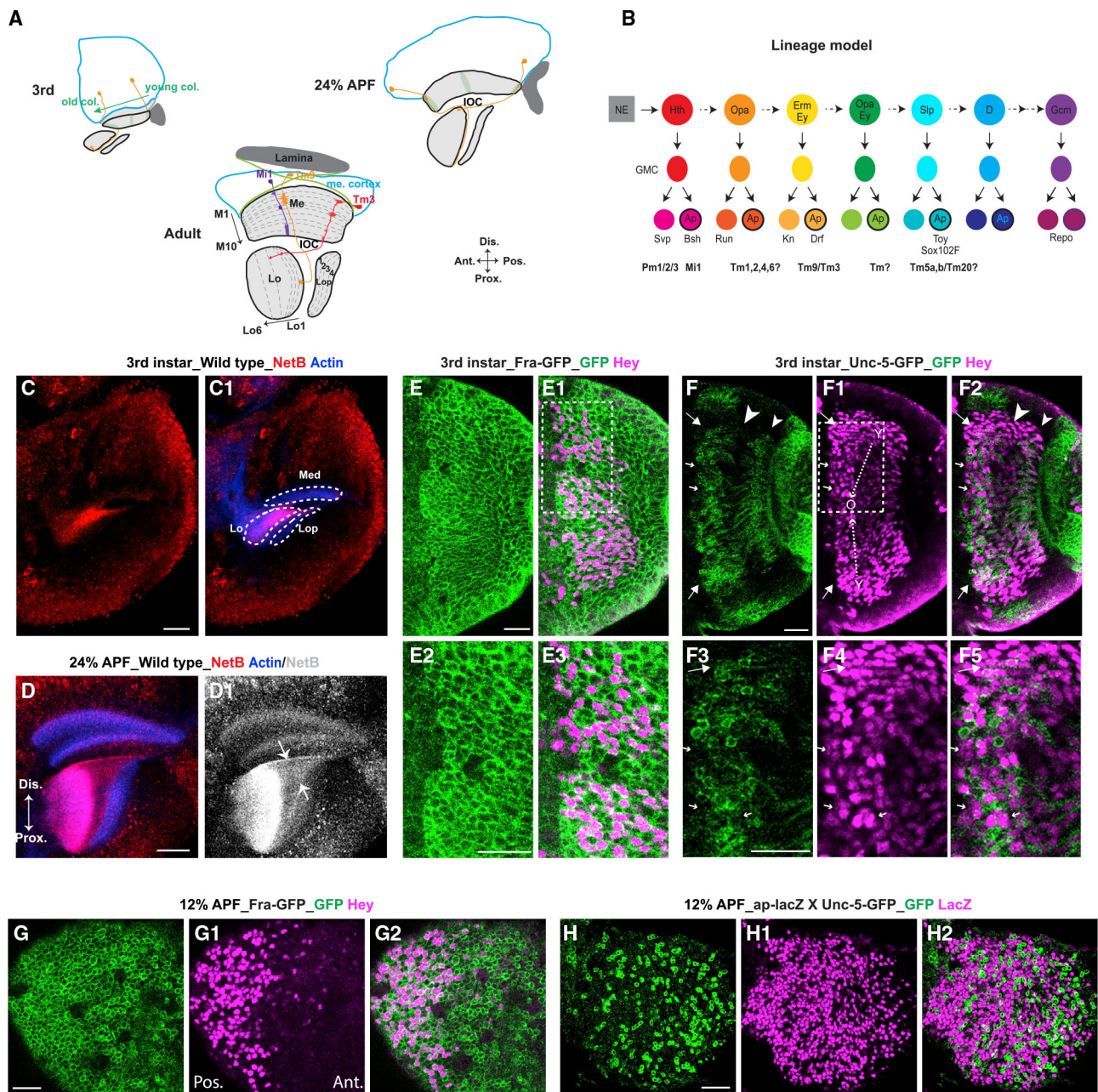


**Figure 1. Netrins, Fra, and Unc-5 are expressed in the optic lobe during development**  
 (A) A schematic drawing of the optic lobe from the third instar larval stage to adult. Individual medulla column is exemplified in green shadow. Me, medulla; Lo, lobula; Lop, lobula plate. At third larval stage, Tm axons from the oldest (anterior earliest-born) medulla columns have arrived at the lobula, but Tm axons from posterior younger columns have not. In early pupal stages, Tm axons from posterior younger columns cross anterior axon bundles to target lobula, forming the IOC. In adult medulla, examples of Tm neurons (Tm3 and Tm9) and Mi neurons (Mi1) are shown.  
 (B) Temporal cascade of medulla neuroblasts and Notch-dependent binary fate choice between sister neurons. Some temporal stages are skipped for simplicity. The Notch-on

daughter from each GMC turns on the expression of Ap. Expression of relevant neural transcription factors and exemplified neural types known before this work are shown. (C and C1) The expression/distribution pattern of NetB (red) in the third instar larval optic lobe. Actin is labeled by phalloidin (blue). Neuropils are outlined. (D and D1) The expression/distribution pattern of NetB (red in D, gray in D1) in the 24% APF larval optic lobe. Actin is labeled by phalloidin (blue). Arrows point to NetB localized in the cleft. (E and E1) The expression patterns of Fra-GFP (green) and Hey (purple), in the third larval optic lobe.

(E2 and E3) Magnified views of the outlined rectangle in (E1).

(F–F2) The expression patterns of Unc-5-GFP (green) and Hey (purple) in the third larval optic lobe. Young Notch-on (Hey+) and Notch-off (Hey–) neurons express Unc-5 (big arrow), while old Ap+ neurons turn off Unc-5 expression (small arrows). The big white arrowhead indicates a gap in Unc-5 expression in medulla neurons born in middle temporal stages. The small arrowhead indicates Unc-5 expression in Mi1 neurons born in the first temporal stage.

(F3–F5) Magnified views of the outlined rectangle in (F1).

(G–G2) The expression patterns of Fra-GFP (green) and Hey (purple) in the 12% APF pupal optic lobe. All Notch-on neurons express Fra.

(H–H2) The mutual exclusive expression patterns of Unc-5-GFP and *ap*-LacZ in the 12% APF pupal optic lobe.

Scale bars, 20  $\mu$ m.

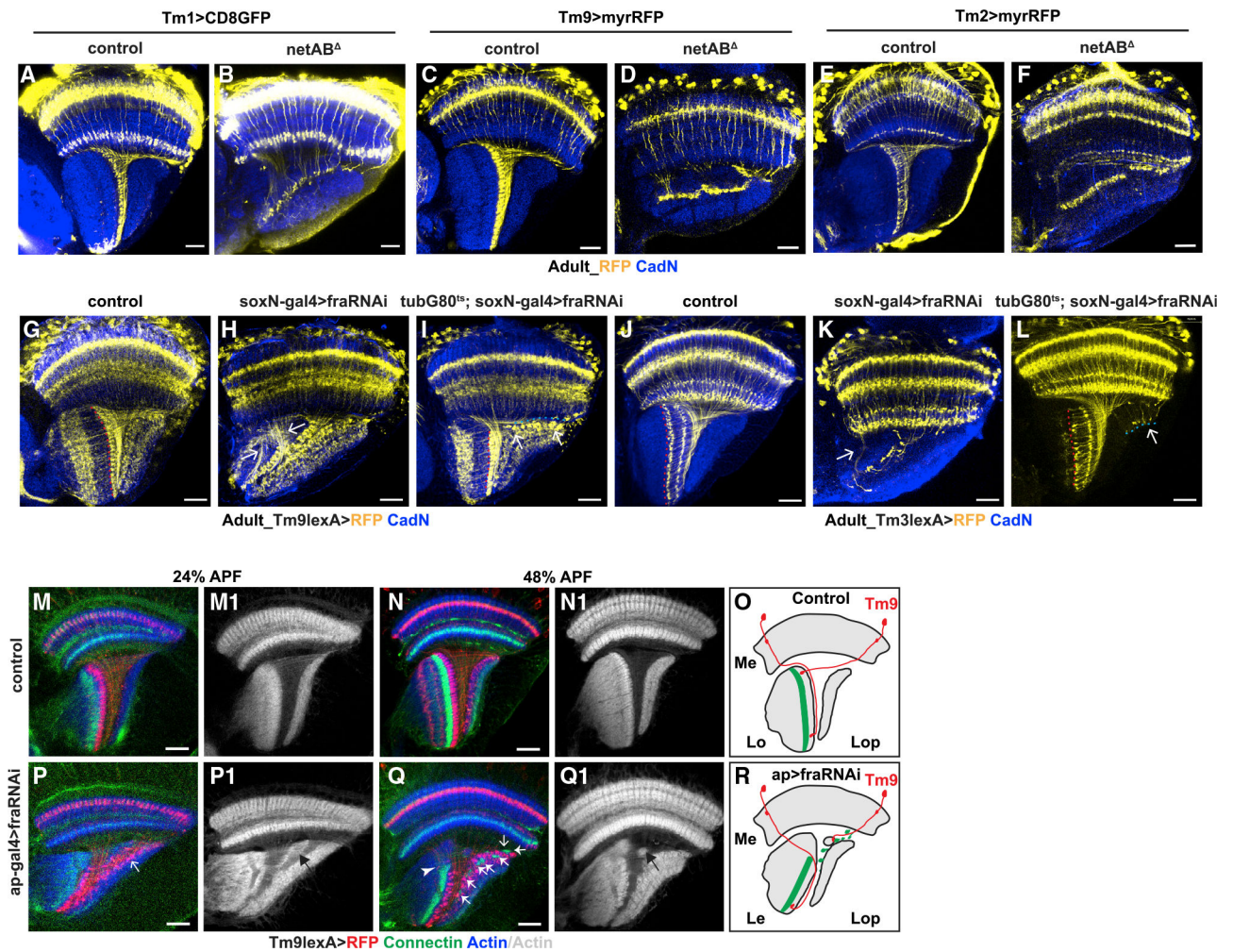


**Figure 2. Netrin signaling regulates IOC formation**

(A, C, and E) Tm1 (A), Tm9 (C), and Tm2 (E) in wild type.

(B, D, and F) Tm1 (B), Tm9 (D), and Tm2 (F) in *netAB* mutants. The X-shaped IOC structure is disrupted in *netAB* mutants, while the targeting layers of Tm1, Tm9, and Tm2 are not affected. CadN (blue) labels all neuropils.

(G) Tm9 in wild type. Note this driver labels other neural types besides Tm9, and Tm9 axons terminate at distal lobula (outlined).

(H) Tm9 in *SoxN-Gal4>fraRNAi*. IOC is disrupted (arrows).

(I) Knocking down Fra in late-born medulla columns only affects Tm9 targeting in late-born columns (blue dashed line, arrows).

(J) Tm3 in wild type.

(K) Tm3 in *SoxN-Gal4>fraRNAi*. IOC is disrupted.

(L) Knocking down Fra in late-born medulla columns only affects Tm3 targeting in late-born columns (arrow, blue dashed line).

(M–R) Targeting of Tm9 axons and neuropil structure in wild type (M–O) and *ap-Gal4>fraRNAi* (P–R) brains at 24% APF (M and P), or 48% APF (N and Q) at 29°C.

Tm9LexA>RFP is in red, Connectin is in green, and Actin is in blue in (M, N, P, and Q).

Actin is in gray in (M1, N1, P1, and Q1). Note that this *lexA* driver also labels other neural types. The Tm9 axon terminal is cylinder shaped.

(M–N1) In wild type, Tm9 axons terminate at Lo1, neuropils are intact, and Connectin labels Lo3 and the distal half of Lo4.

(O) Schematic of Tm9 in wild type at 48% APF.

(P–Q1) In *ap-Gal4>fraRNAi* brains, Tm9 axon terminals are mislocated to the surface of the lobula plate (arrow in P); lobula organization is damaged (black arrows in P1 and Q1); The Connectin band is discontinuous at lobula (arrowhead in Q) and accompanies mislocated Tm9 terminals (arrows in Q).

(R) Schematic of Tm9 in *ap>fraRNAi*. Tm9 from late-born columns do not cross early-born Tm axons but stop half-way. Mislocated Tm9 axon terminals still mature and are accompanied with Connectin signals.

Scale bars, 20  $\mu\text{m}$ .

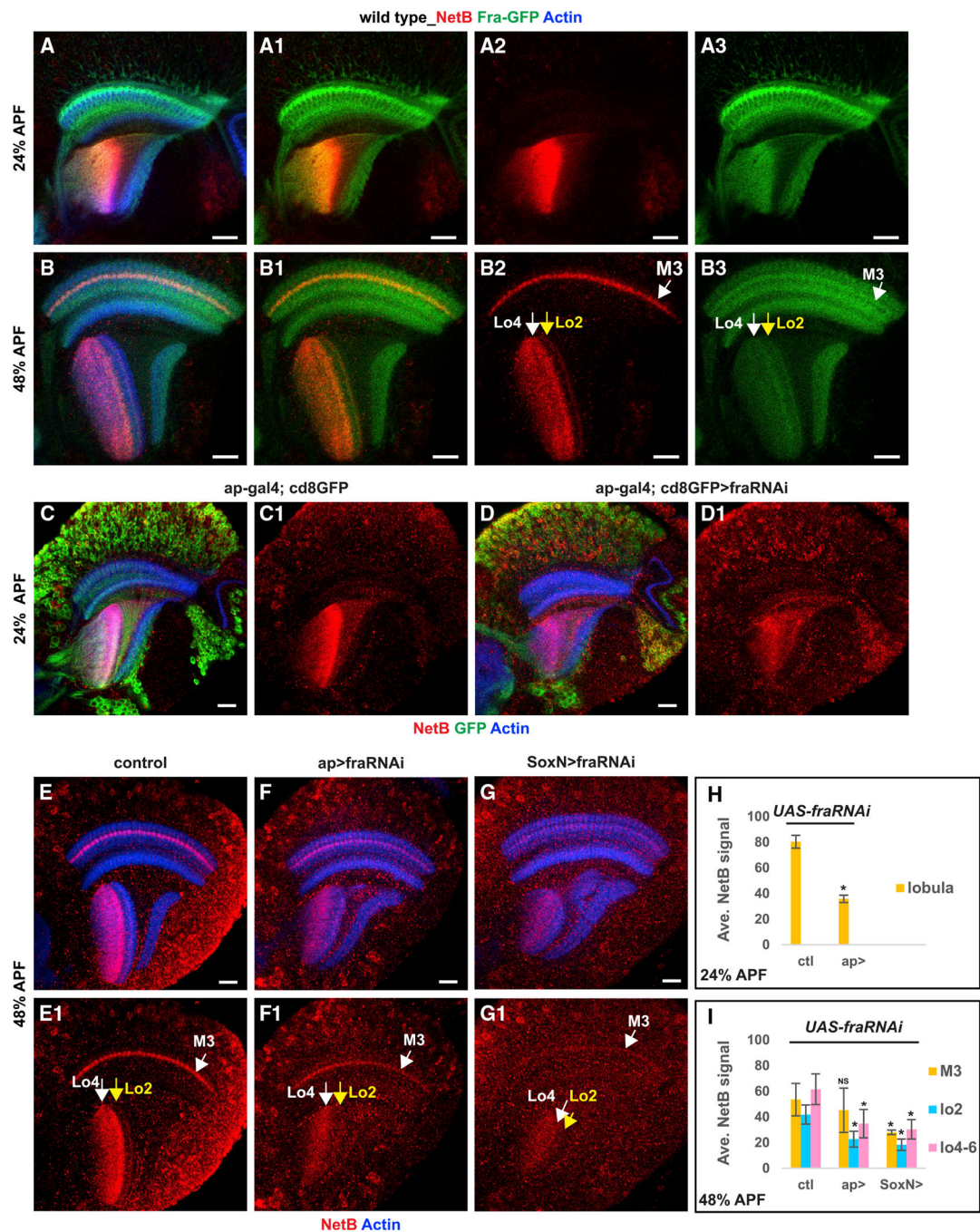


**Figure 3. Fra from medulla neurons regulates NetB distribution**

(A–A3) Fra-GFP (green) and NetB (red) are co-stained at 24% APF. Fra-GFP and NetB are colocalized at lobula. Actin (blue) is used to label all neuropils.

(B–B3) Fra-GFP (green) and NetB (red) are co-stained at 48% APF. All NetB-enriched areas (M3, Lo2, and Lo4–6) are colocalized with Fra-GFP.

(C–D1) 24% APF brains are shown. NetB is in red.

(C and C1) Control: ap-Gal4>*UAScd8GFP* (green) labels half of the neurons in optic lobe.

(D and D1) Knocking down Fra using *ap-Gal4*. The NetB signal in the medulla cortex is normal. The NetB level at lobula is reduced compared with control.

(E–G1) 48% APF brains are shown. NetB is in red.

(E and E1) Control. NetB-enriched layers are shown.

(F and F1) Knocking down Fra by *ap-Gal4*. M3 NetB level is not significantly affected. Lo2 NetB and Lo4–6 NetB are greatly reduced.

(G and G1) Knocking down Fra by *SoxN-Gal4*. NetB enrichment at M3, Lo2, and Lo4–6 is greatly reduced.

(H) Quantification of (C–D1).  $n = 5$  for control or test group. The decrease of NetB level in *ap-Gal4>FraRNAi* lobula is significant (t test:  $p = 2.17 \times 10^{-8}$ ). Data are represented as mean  $\pm$  SEM.

(I) Quantification of (E–G1).  $n = 7$  for control,  $n = 5$  for test groups. Average NetB levels at M3, Lo2, and Lo4–6 in *ap-Gal4>fraRNAi* or *SoxN-Gal4>fraRNAi* optic lobes are compared with corresponding regions in control. Asterisks indicate significant reductions (t test: for M3 NetB,  $p = 0.44$  for *ap-Gal4>fraRNAi*,  $p = 0.002$  for *SoxN-Gal4>fraRNAi*; for Lo2 NetB,  $p = 0.002$  for *ap-Gal4>fraRNAi*,  $p = 0.001$  for *SoxN-Gal4>fraRNAi*; for Lo4–6 NetB,  $p = 0.007$  for *ap-Gal4>fraRNAi*,  $p = 0.002$  for *SoxN-Gal4>fraRNAi*). Data are represented as mean  $\pm$  SEM.

Scale bar, 20  $\mu\text{m}$ .

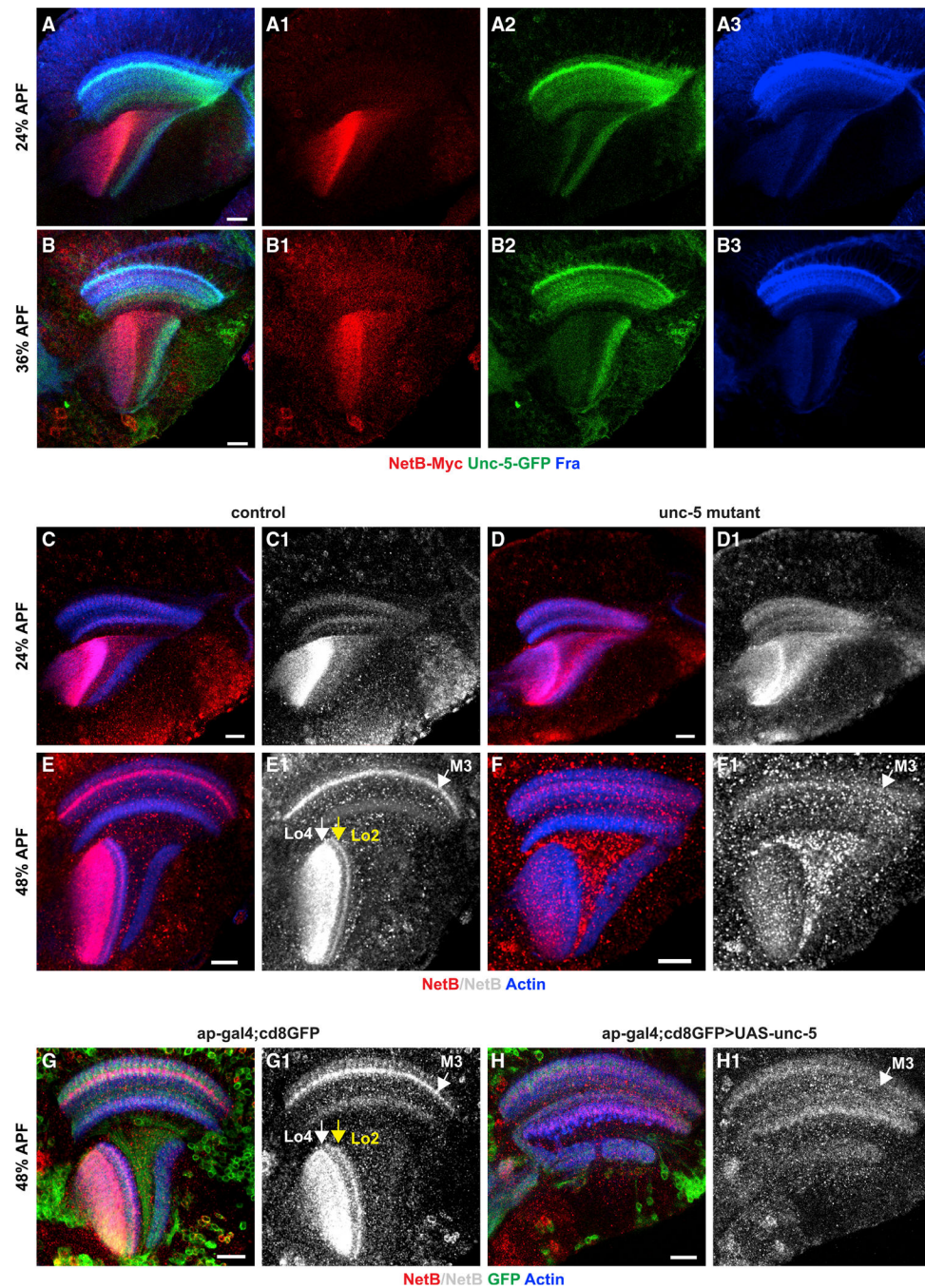


#### Figure 4. *Unc-5* plays a role in NetB distribution

(A–A3) *Unc-5*-GFP (green), Fra (blue), and NetB-Myc (red) are co-stained at 24% APF. *Unc-5* level is high in lobula plate and medulla, while NetB level is high in lobula.

(B–B3) *Unc-5*-GFP (green), Fra (blue), and NetB-Myc (red) are co-stained at 36% APF.

(C–D1) 24% APF brains.

(C and C1) NetB (red in C and gray in C1) distribution in wild type.

(D and D1) NetB distribution in *unc-5* mutants. NetB is also enriched in lobula plate and medulla.



(E–F1) 48% APF brains.

(E and E1) NetB distribution in wild type.

(F and F1) NetB distribution in *unc-5* mutants. M3 NetB (white arrow) is almost gone; lobula NetB level is greatly reduced; high-intensity dots of NetB signal are observed throughout the optic lobe, especially in the cleft between neuropils.

(G–H1) 48% APF brains.

(G and G1) NetB distribution in wild type.

(H and H1) Overexpression of *Unc-5* using *ap-Gal4*. Lobula complex is severely damaged. No NetB is enriched at lobula complex. M3 NetB (white arrow) is greatly reduced. Actin is used to label all neuropils.

Scale bar, 20  $\mu$ m.

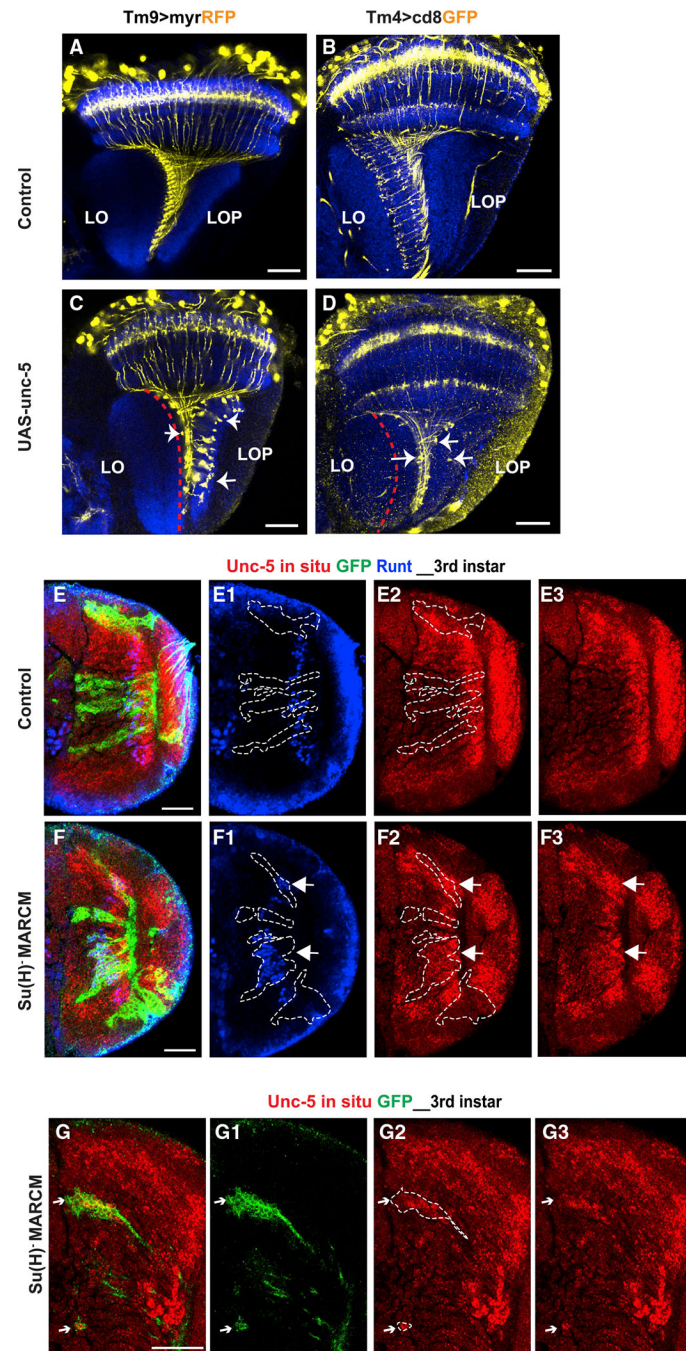


### Figure 5. Notch signaling regulates *Unc-5* expression in the medulla

(A–D) Overexpression of *Unc-5* leads to mistargeting of Tm axons using Tm9 and Tm4 as examples. Actin is labeled by phalloidin (blue). Red lines mark where the corresponding Tm neurons terminate in the wild type. Arrows point to the mistargeted axon terminals.

(A and C) Tm9-Gal4 driving UAS-myRFP (yellow) in control (A) or UAS-*Unc-5* (C) brains. (B and D) Tm4-Gal4 driving UAS-cd8GFP (yellow) in control (B) or UAS-*Unc-5* (D) brains. (E–G3) *In situ* hybridization with *Unc-5* probe (red) in control (E–E3) or *Su(H)* mutant clones (F–G3) marked by GFP (green). In control brains (E–E3), Runt<sup>+</sup> neurons (blue) are

arranged in a salt-and-pepper manner (E1). In *Su(H)* mutant clones (F–F3), Runt+ neurons (blue) are compacted in mutant clones (F1, white arrow) and ectopic Unc-5 signals are also compacted in these clones (F2 and F3). However, not all mutant clones show ectopic Unc-5 signals. In late-born neurons (G–G3), compacted strong Unc-5 mRNA signal is observed in *Su(H)* mutant clones (arrows).

Scale bars, 20  $\mu\text{m}$ .

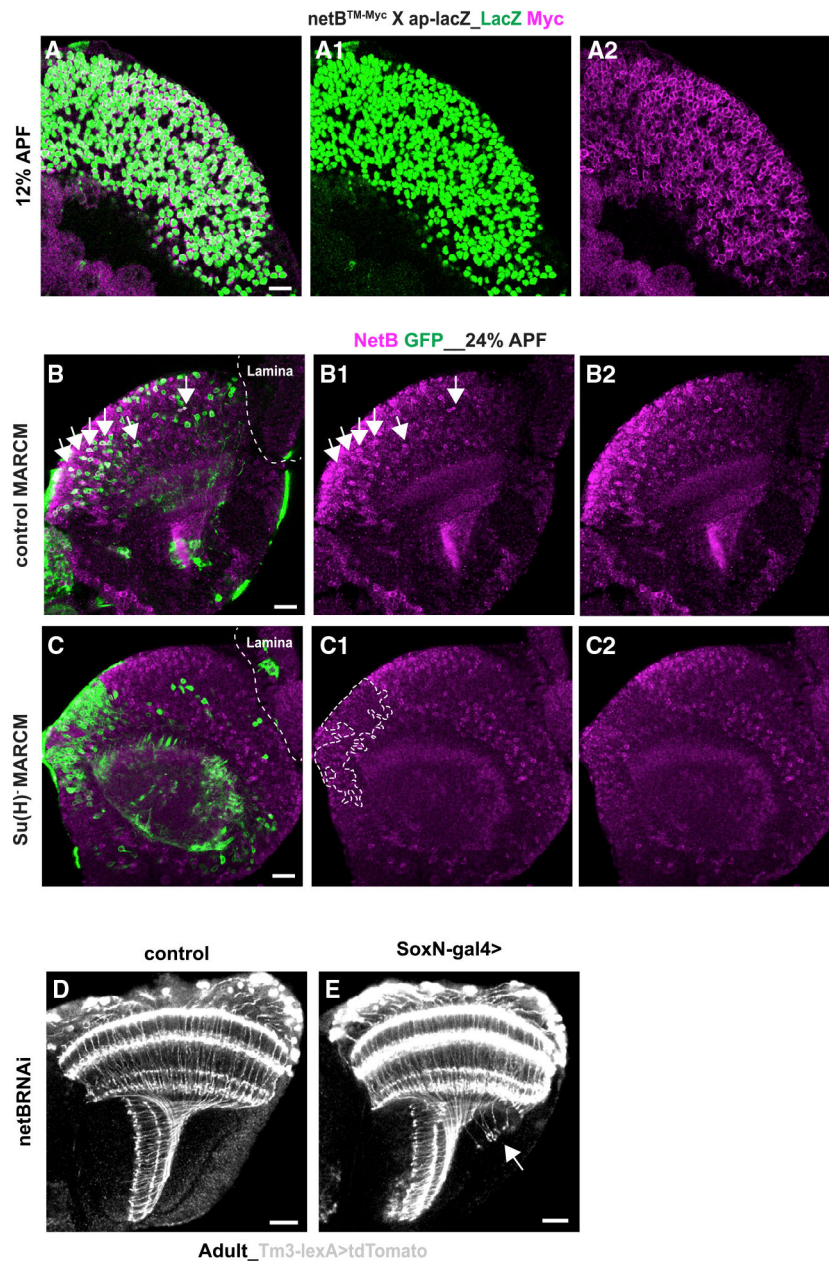


### Figure 6. Notch signaling regulates NetB expression in medulla neurons

(A–A2) NetB-Myc (purple) is co-stained with ap-lacZ (green), which is activated in Notch-on neurons of medulla. All NetB-expressing medulla neurons are Notch-on.

(B–C2) MARCM is used to create control clones (B–B2) or *Su(H)* mutant clones (C–C2) marked by GFP (green). NetB protein (purple) is observed.

(B–B2) NetB staining is observed in control clones (white arrows).

(C–C2) *Su(H)* mutant clones do not show any NetB staining.

(C1) Big *Su(H)* clones are outlined.

(D and E) Tm3-LexA driving tdTomato (gray) in control (D) or *SoxN-Gal4>netBRNAi* (E) brains. *SoxN-Gal4* is expressed in medulla neuroblasts and inherited by progenies.

Knocking down NetB in medulla neurons affects Tm3 targeting from late-born columns (arrow).  
Scale bars, 20  $\mu$ m.

Author Manuscript

Author Manuscript

Author Manuscript

Author Manuscript

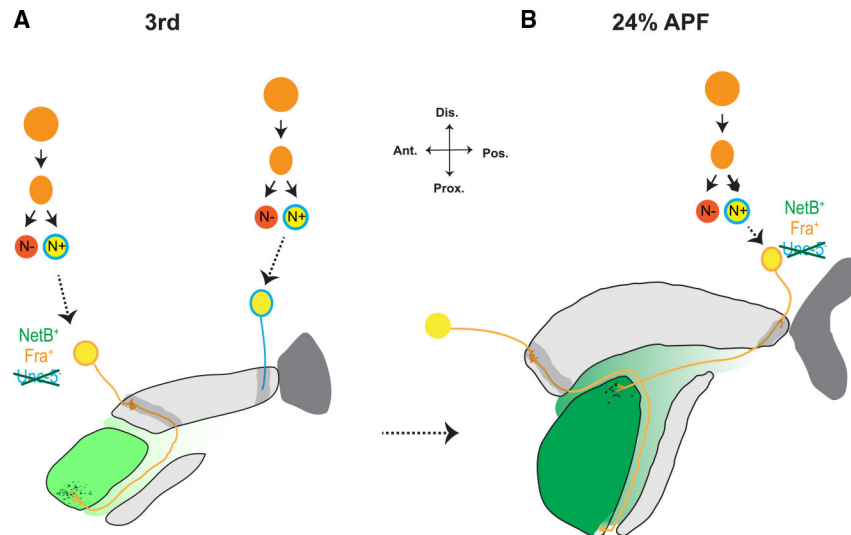


**Figure 7. Model of the regulation of Netrin pathway components by Notch-dependent binary fate choice**

(A) In Tm neurons derived from the Notch-on hemilineage, Notch signaling is required to turn off *Unc-5* during axon targeting. This enables Tm axons to target lobula. Notch signaling is also required to activate *NetB* expression in these Tm neurons.

(B) *NetB* derived from Tm neurons of early-born (anterior) medulla columns contribute to the *NetB* pool in the lobula and is required for Tm axons from late-born (posterior) medulla columns to form the IOC and target the lobula.

## KEY RESOURCES TABLE

REAGENT or RESOURCE	SOURCE	IDENTIFIER
Antibodies		
Mouse anti-Connectin	DSHB	Cat# C1.427; RRID:AB_10660830
Mouse anti-Cut	DSHB	Cat# 2B10; RRID:AB_528186
Rat anti-Dfr	M. Sato	N/A
Rat anti-DN-Cadherin	DSHB	Cat# DN-Ex#8; RRID:AB_528121
Rabbit anti-Fra	Y.N. Jan	N/A
Sheep anti-GFP	AbD Serotec	Cat# 4745-1051; RRID:AB_619712
Rabbit anti-HA	Cell Signaling Technology	Cat# 3724; RRID:AB_1549585
Guinea pig anti-Hey	C. Delidakis	N/A
Chicken anti-LacZ	Abcam	Cat# ab9361; RRID:AB_307210
Mouse anti-Myc	DSHB	Cat# 9E10; RRID:AB_2266850
Rabbit anti-NetA	B.Altenein	N/A
Rabbit anti-NetB	B.Altenein	N/A
Phalloidin-iFluor 405	Abcam	Cat# ab176752; N/A
Rabbit anti-RFP	Abcam	Cat# ab62341; RRID:AB_945213
Guinea-pig anti-Runt	C. Desplan	N/A
Donkey Anti-Chicken 647	Jackson ImmunoResearch Laboratories Inc.	Cat# 703-605-155; RRID:AB_2340379
Donkey Anti-Guinea Pig Cy3	Jackson ImmunoResearch Laboratories Inc.	Cat# 706-165-148; RRID:AB_2340460
Donkey Anti-Guinea Pig 488	Jackson ImmunoResearch Laboratories Inc.	Cat# 706-545-148; RRID:AB_2340472
Donkey Anti-Guinea Pig 647	Jackson ImmunoResearch Laboratories Inc.	Cat# 706-605-148; RRID:AB_2340476
Donkey Anti-Mouse 488	Jackson ImmunoResearch Laboratories Inc.	Cat# 715-545-151; RRID:AB_2341099
Donkey Anti-Mouse Cy5	Jackson ImmunoResearch Laboratories Inc.	Cat# 715-175-151; RRID:AB_2340820
Donkey Anti-Mouse Cy3	Jackson ImmunoResearch Laboratories Inc.	Cat# 715-165-151; RRID:AB_2315777
Donkey Anti-Sheep 488	Jackson ImmunoResearch Laboratories Inc.	Cat# 713-545-147; RRID:AB_2340745
Donkey anti-Rabbit 555	Molecular Probes (Thermo Fisher)	Cat# A-31572; RRID:AB_162543
Donkey Anti-Rabbit 488	Jackson ImmunoResearch Laboratories Inc.	Cat# 711-545-152; RRID:AB_2313584
Donkey Anti-Rat Cy3	Jackson ImmunoResearch Laboratories Inc.	Cat# 712-165-153; RRID:AB_2340667
Donkey Anti-Rat Cy5	Jackson ImmunoResearch Laboratories Inc.	Cat# 712-175-153; RRID:AB_2340672
Chemicals, peptides, and recombinant proteins		
SlowFade Gold	Thermo Scientific	S36936
Deposited data		

REAGENT or RESOURCE	SOURCE	IDENTIFIER
The published scRNA-seq data	Kurmangaliyev et al., 2020 <sup>29</sup>	GEO: GSE156455
Experimental models: Organisms/strains		
<i>netA</i> <i>B<sup>myc</sup></i>	B. J. Dickson	N/A
<i>netA</i> <i>B</i>	B. J. Dickson	N/A
<i>UAS-netBRNAi</i>	3DSC	25861
<i>unc-5-GFP</i>	BDSC	64547
<i>unc-5<sup>8</sup></i>	G. J. Bashaw	N/A
<i>UAS-HA-unc-5</i>	G. J. Bashaw	N/A
<i>UAS-unc-5 RNAi</i>	BDSC	33756
<i>fra-GFP</i>	BDSC	59835
<i>UAS-fra RNAi</i>	BDSC	40826
<i>FRTG13, fra<sup>3</sup></i>	BDSC	8813
<i>FRT40A, Su(H)<sup>47</sup>/CyO</i>	F. Schweisguth	N/A
<i>Mi{FlpStop}apMI01996-FlpStop.ND/CyO</i>	BDSC	67675
<i>UAS-NICD</i>	Gary Struhl	N/A
<i>numb<sup>15</sup> FRT40A/CyO</i>	F. Schweisguth	N/A
<i>ap-Gal4/CyO</i>	Barbara et al., 1992 <sup>43</sup>	N/A
<i>ap-lacZ</i>	Barbara et al., 1992 <sup>43</sup>	N/A
<i>elav-Gal4; UAS-Dcr2</i>	BDSC	25750
<i>til-Gal4</i>	BDSC	49694
<i>SoxN-Gal4</i>	BDSC	GMR41H10
<i>27b-Gal4</i>	Morante and Desplan, 2008 <sup>20</sup>	N/A
<i>Tm2: Otd-gal4</i>	Morante and Desplan, 2008 <sup>20</sup>	N/A
<i>Adult: Tm3-Gal4</i>	BDSC	48569
<i>Larval: Tm3-Gal4</i>	BDSC	76324
<i>Tm3-LexA</i>	BDSC	52459
<i>Tm4-Gal4</i>	BDSC	49922
<i>Tm9-Gal4</i>	BDSC	48050
<i>Tm9-LexA</i>	BDSC	54982
<i>UAS-myrRFP</i>	BDSC	7118
<i>MCFO</i>	BDSC	64085
<i>y,w,hsFLP,UAS-CD8::GFP; FRT40A, tub-Gal80; tub-Gal4/TM6B</i>	Liquan Luo	N/A
Oligonucleotides		
Unc-5 probe with Quasar <sup>®</sup> 570 Dye	LGC Biosearch Technologies	SMF-1063-5
Software and algorithms		
Zen	Carl Zeiss	<a href="https://www.zeiss.com/microscopy/en/products/software/zeiss-zen.html">https://www.zeiss.com/microscopy/en/products/software/zeiss-zen.html</a>
R (version 4.0.3)	CRAN	<a href="https://www.r-project.org/">https://www.r-project.org/</a>



---

<b>REAGENT or RESOURCE</b>	<b>SOURCE</b>	<b>IDENTIFIER</b>
Seurat (version 3.2.3)	N/A	<a href="https://satijalab.org/seurat/">https://satijalab.org/seurat/</a>
Photoshop 2021	Adobe	<a href="https://www.adobe.com/cy_en/products/photoshop.html">https://www.adobe.com/cy_en/products/photoshop.html</a>
Illustrator 2021	Adobe	<a href="https://www.adobe.com/products/illustrator.html">https://www.adobe.com/products/illustrator.html</a>

---

Author Manuscript

Author Manuscript

Author Manuscript

Author Manuscript